Ion-Trapping Saturation of the Brillouin Instability

Christopher E. Clayton, Chan Joshi, and Francis F. Chen
Electrical Engineering Department, University of California, Los Angeles, California 90024
(Received 18 August 1983)

The ion acoustic wave and harmonics driven by stimulated Brillouin scattering are probed by space- and time-resolved ruby-laser Thomson scattering. Corresponding to the 6% backscatter observed, the ion wave is seen to saturate at (5–10)% amplitude, a level quantitatively predictable from the nonlinear frequency shift caused by ion trapping.

PACS numbers: 52.35.Mw, 52.35.Dm, 52.40.Db

The saturation level of parametric instabilities, particularly stimulated Brillouin scattering (SBS), has received a great deal of attention because of the potential limitation to energy coupling in laser fusion targets. Though SBS reflectivities R of 50% or higher have been seen,[1,2] several studies in underdense plasmas have revealed a plateau[2] or saturation[3-6] at a surprisingly low level of 5%–10%. Detailed probing of the ion wave shows that this level is explained by a change in the spatial structure of the ion wave caused by ion trapping, not by harmonic generation, and suggests that R can be driven beyond this plateau by sufficient pump power.

For our experimental parameters,[7] we use the theory of convective SBS from heavily damped ion waves in a finite-length, homogeneous plasma.[8] Let the interaction occur in $0<z<L$, where z increases in the direction of the laser beam $(\omega_0, \vec{k}_0)$. The balance between damping and ponderomotive drive then gives for the peak ion-wave amplitude[7]

$$\tilde{n}(z)/n_0 = (4/k_0)(n_c/n_0)K_{g0}R^{1/2}(z), \quad (1)$$

where the local reflectivity $R(z)$ exponentiates from the noise level $R_N(L)$ as

$$R(z) = R_N(L)\exp[2K_{g0}(L-z)], \quad (2)$$

and K_{g0} is the spatial growth rate[7]

$$K_{g0} = (2\pi/\omega_0)(e/mc^2)^2(\Omega_p^2/\omega_i\gamma_i)I_0. \quad (3)$$

Thus $\tilde{n}(z)$ is expected to exponentiate toward the laser at a rate proportional to pump intensity I_0 and the distance from the noise source. Here the ion wave has frequency ω_i and damping rate γ_i, the (nitrogen) ion plasma frequency is Ω_p, and the ratio n_0/n_c of background electron density to critical density is[9] about 0.02. At this density, the ion wave has $k_i \simeq 2k_0$, and the k-matching angle for collective Thomson scattering with 6943-Å ruby light is 7.5°.

That the scattered light came from Brillouin-driven ion waves was confirmed numerous ways. First, the scattered ruby light grew exponentially with pump power [the circles in Fig. 1(a)] with the same slope as the measured SBS light [the solid line in Fig. 1(a)]. Second, as shown in Fig. 1(b), the ruby light was red shifted or blue shifted when k-matched to $+2\vec{k}_0$ or $-2\vec{k}_0$, respectively, by the same 10-GHz frequency shift as was seen in the SBS light at 10.6 μm. Third, the scattered ruby light was sharply collimated near 7.5°, indicating that k_i had a discrete spectrum at $2k_0$. Fourth, a 1° rotation of $\vec{k}_i$ relative to the ruby scattering system drastically reduced the scattered power, indicating that the ion waves were nearly planar. Fifth, the ruby scattering occurs in 1–2-nsec bursts, matching the SBS behavior.[9] These were *local* measurements, so that the

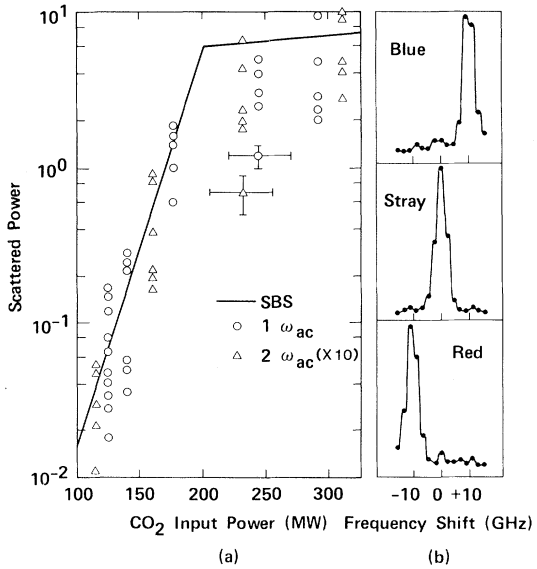

FIG. 1. (a) Thomson-scattered power at the fundamental (circles) and second harmonic (triangles) of the SBS ion wave vs pump power. The solid line summarizes previous data on SBS reflectivity. (b) Spectra of Thomson-scattered ruby light when k-matched to $+2k_0$ (red shift) and $-2k_0$ (blue shift). The "stray" curve shows the instrument width.

points on Fig. 1(a) show that the ion-wave amplitude at a particular point in the interaction region saturated as the CO_2 pump power was increased. [The CO_2 (ruby) beam had 40 (20) nsec full width at half maximum, 0.3 (0.5) mm spot size, and 1 (1) cm focal depth.]

To probe the entire ion wave, cyclindrical optics were used to focus the ruby beam into a line 1 cm long overlapping the focal volume of the CO_2 pump. Light scattered at 7.5° was imaged with unit magnification onto the slit of a streak camera. The spatial resolution of the system was measured with suitable masks to be better than 300 μm, or about $\frac{1}{20}$ of the interaction length. The intensity variation across the slit, therefore, gives a one-dimensional image of the ion-wave intensity, which was then streaked in time, resulting in data such as shown in Fig. 2(a). This streak picture shows the characteristic pulsing of the ion wave in time (probably due to fluctuations in the noise source) and also the lengthening of the interaction region in the $-\vec{k}_0$ direction due to laser ionization and heating. Figure 3 shows time scans at various positions z, from a similar streak image. The fastest decay rates thus observed must be representative of the natural damping rate of the ion waves. This decay rate would obtain if either the pump or the acoustic noise were to go rapidly to zero. We find that the fastest decay rates give $\gamma_i/\omega_i \simeq 0.1$, which is consistent with Landau damping for $ZT_e/T_i = 4$, a value obtained from ω_i and Saha equilibrium.

Scanning the streak images in the spatial direction yields the ion-wave intensity profiles shown in Figs. 2(b)–2(d). According to Eqs. (1) and (2), the logarithm of $\tilde{n}$ should grow linearly from the noise level at the downstream (right-hand) side to the upstream end of the interaction region. Figure 2(b) approaches this idealized condition. Figure 2(c), however, shows a case where at different times the ion wave grows at the same rate in space but saturates for different distances as the plasma expands. In Fig. 2(d), the ion wave starts out flat topped (saturated) but later in time reverts to an exponential profile with a small slope. The apparently random variation in these profiles is probably due to fluctuations partly in the pump intensity and partly in the nonthermal noise level.

The profiles exhibiting a flat top in Figs. 2(c) and 2(d) are accompanied by large slopes in the downstream region, indicating a high pump power. The difference in slopes in the downstream growth region and the upstream flat-top region cannot be caused by a change in plasma or pump parameters due for instance, to, filamentation, because this cannot be large enough to give rise to such a large change in slope [Eq. (3)]. Rather, the change in slope suggests a nonlinearity in the ion wave itself at large amplitudes. The amplitude at the onset of saturation [e.g., at 450 psec in Fig. 2(d)] can be determined by evaluating the space-dependent Bragg scattering formula [essentially Eq. (1) if $\tilde{n}(z)$ is exponential] with the value of K_{g0} measured in Fig. 2, and setting $R(0)$ equal to the 6% measured SBS power reflectivity. This gives $n/n_0 = 5\%$–10%, with the uncertainty due to two-dimensional effects.[9] The measured value of K_{g0} agrees with that computed from Eq. (3).

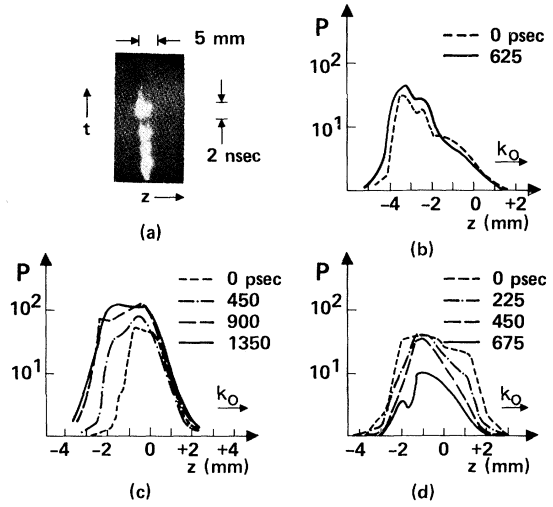

FIG. 2. (a) Typical streak image at 15-nsec full frame. (b)–(d) Microdensitometer scans of streak images of three shots showing relative scattered power $P \propto (\tilde{n}/n_0)^2$ vs z at various times during the pulse. One acoustic period is $\simeq 100$ psec. The CO_2 best focus is at $z = 0$.

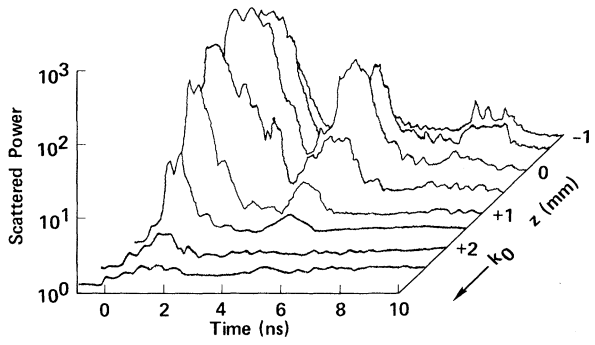

FIG. 3. Microdensitometer scan showing time behavior at various positions.

We now show that 5%–10% amplitude is sufficient to cause a trapping nonlinearity. A resonant ion with $v_{\parallel} \equiv \vec{k}_i \cdot \vec{v} \simeq \omega_i/k_i$ can be trapped if its bounce time is less than the time needed to diffuse by collisions out of the resonant zone in $v_{\perp}$-$v_{\parallel}$ space. Since diffusion parallel to the ions' original velocity is generally slower than that perpendicular to it,[10] the ions trapped first will be those with thermal velocities near ω_i/k_i in the direction of $\vec{k}_i$. From such considerations, we find[11] a trapping threshold of $\tilde{n}/n_0 \simeq 5\%$. The number of trapped ions increases to 2% at $\tilde{n}/n_0 \simeq 11\%$. The inferred saturation amplitudes are thus consistent with the onset of ion trapping.

To see how a 2% trapped-ion population can cause saturation, we recall that the extra density of the trapped species in the wave troughs causes a nonlinear frequency shift[12] asymptotically after many bounce times. For equal phase and group velocities $v_p = v_g = c_s$, this shift is[12]

$$\Delta\omega/\omega_i \simeq v_p{}^3 f_0''(v_p)(\tilde{n}/n_0)^{1/2}, \tag{4}$$

where ω_i is the linear frequency and $f_0''(v_p)$ is the second derivative of the normalized ion distribution function at $v = v_p$. This shift occurs locally upstream of the point where $\tilde{n}/n_0$ exceeds the trapping threshold of 5%. In the upstream region, therefore, the natural phase velocity has the nonlinear value V_{NL}, different from the linear value c_s in the downstream region, while k_i is still fixed at $2k_0$. Since the backscattered light wave E_2 has grown in the linear region, it has the wrong frequency shift to drive the large-amplitude wave resonantly in the upstream region. By assuming a discontinuous jump from c_s to V_{NL} in the two regions, we can obtain an expression for the spatial growth rate K_g in the saturated region. The nonresonantly driven ion wave follows the equation

$$\left(\frac{\partial^2}{\partial t^2} + 2\gamma_i \frac{\partial}{\partial t} - V_{\mathrm{NL}}{}^2 \frac{\partial^2}{\partial z^2}\right)\tilde{n} = -\frac{\partial}{\partial z}\frac{F_{\mathrm{NL}}}{M}, \tag{5}$$

where F_{NL} is the ponderomotive force with the *linear* frequency ω_i due to the pump beating with E_2. Since $\tilde{n}$ must have the same frequency as the driving term, we can solve Eq. (5) for $\tilde{n}$ and substitute the result into the driven wave equation for E_2 to find the growth rate

$$K_g = K_{g0}\Gamma[(\xi^2 - 1)^2 + \xi^2\Gamma^2]^{1/2} \times \cos\left[\frac{\pi}{2} - \tan^{-1}\left(\frac{\xi\Gamma}{1-\xi^2}\right)\right], \tag{6}$$

where K_{g0} is given by Eq. (3) and $\xi \equiv \omega_i/2k_0V_{\mathrm{NL}}$, $\Gamma \equiv \gamma_i/k_0V_{\mathrm{NL}}$. To compare with theory, we write $V_{\mathrm{NL}} = (\omega_i + \Delta\omega)/2k_0$, so that $\xi^{-1} = 1 + (\Delta\omega/\omega_i)$. For $\Gamma \simeq 0.2$, Eq. (6) shows that a 30% reduction in V_{NL} ($\Delta\omega/\omega_i = -0.3$) reduces $2K_{g0}$ by an order of magnitude. The backscattered wave generated downstream then passes through the upstream region with very little gain. This reduction in growth length accounts for the flat-topped profiles of Fig. 2(c) and the saturation region of Fig. 1(a). From Eq. (4) we find that $\Delta\omega/\omega_i = -0.3$ implies $\tilde{n}/n_0 \simeq 10\%$, in agreement with the value inferred from the data. Though Eq. (4) was derived for collisionless plasmas with moderate ZT_e/T_i, adding collisions and reducing ZT_e/T_i are offsetting effects.

Other possible saturation mechanisms are ion heating and harmonic generation. Estimates of ion heating[13,14] give saturated values of R in excess of 50% for $L/\lambda_0 > 500$, as in this experiment, and cannot explain values of R less than 10%. Saturation by harmonic generation has been suggested by many theorists, and indeed changing the scattering angle allows us[9] and others[6] to detect several harmonics at $(n\omega_i, n\vec{k}_i)$. The harmonics have a discrete spectrum, with intensities $\propto 10^{-n}$; there is no turbulence. As the triangles in Fig. 1(a) show, the harmonics do not grow relative to the fundamental; consequently, they cannot be responsible for the observed saturation. We believe that they are artifacts of a nonsinusoidal ponderomotive drive caused by the spatial fine structure of the pump in the focal region.

In conclusion, detailed space- and time-resolved measurements of SBS ion waves show that they saturate at $\tilde{n}/n_0 = 5\%$–10% to cause the observed 6% reflectivity. The saturation level can be explained by ion trapping and nonlinear frequency shift as previously conjectured.[3] Observations of harmonics show that these are unrelated to saturation. For intensities I_0 larger than our maximum of 5×10^{11} W/cm^2, our physical picture suggests that ion trapping would occur over almost the entire interaction length, and thus the instability could evolve into stimulated Compton scattering, leading to a further rise in R at $I_0 > 10^{12}$ W/cm^2, as is seen by others.[2]

We wish to acknowledge the valuable assistance of Dr. S. W. Thomas and Dr. E. M. Campbell. This work was supported by the U. S. Department of Energy under Contract No. DE-AS08-81-DP40163, and the National Science Foundation under Grants No. ECS 80-03558 and No. ECS 81-20933.

[1]B. H. Ripin and E. A. McLean, Appl. Phys. Lett. 34, 809 (1979); F. J. Mayer, G. E. Busch, C. M. Kinzer, and K. G. Estabrook, Phys. Rev. Lett. 44, 1498 (1980).

[2]J. Handke, S. A. H. Rizvi, and B. Kronast, Appl. Phys. 25, 109 (1981).

[3]M. J. Herbst, C. E. Clayton, and F. F. Chen, Phys. Rev. Lett. 43, 1591 (1979).

[4]Z. A. Pietrzyk and T. N. Carlstrom, Appl. Phys. Lett. 35, 681 (1979).

[5]R. Giles and A. A. Offenberger, Phys. Rev. Lett. 50, 421 (1983).

[6]C. J. Walsh and H. A. Baldis, Phys. Rev. Lett. 48, 1483 (1982).

[7]C. E. Clayton, C. Joshi, A. Yasuda, and F. F. Chen, Phys. Fluids 24, 2312 (1981).

[8]D. W. Forslund, J. M. Kindel, and E. L. Lindman, Phys. Fluids 18, 1002 (1975).

[9]C. E. Clayton, C. Joshi, and F. F. Chen, in Laser Interaction and Related Plasma Phenomena (Plenum, to be published), Vol. 6.

[10]L. Spitzer, Jr., *Physics of Fully Ionized Gases* (Interscience, New York, 1967), 2nd ed., p. 130.

[11]C. E. Clayton, Thesis, University of California, Los Angeles, 1983 (unpublished).

[12]H. Ikezi, K. Schwarzeneggar, A. L. Simons, Y. Ohsawa, and T. Kamimura, Phys. Fluids 21, 239 (1978).

[13]W. L. Kruer, Phys. Fluids 23, 1273 (1980).

[14]F. F. Chen, C. Joshi, C. E. Clayton, B. Amini, and H. C. Barr, in *Proceedings of the U.S.–Japan Seminar on Theory and Application of Multiply-Ionized Plasmas Produced by Laser and Particle Beams, Nara, Japan* (Osaka University, Japan, 1982), p. 243.

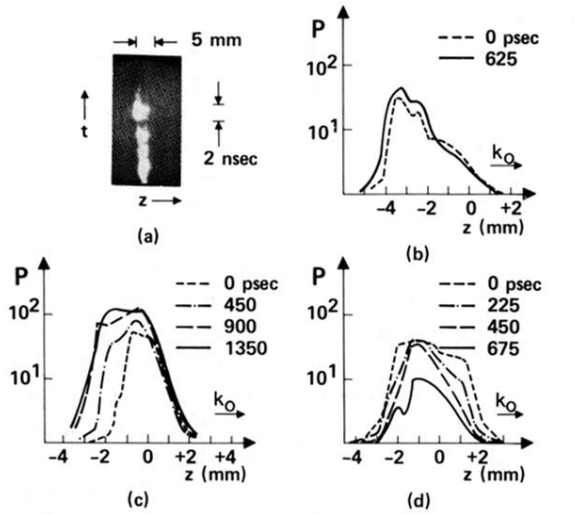

FIG. 2. (a) Typical streak image at 15-nsec full frame. (b)–(d) Microdensitometer scans of streak images of three shots showing relative scattered power $P \propto (\tilde{n}/n_o)^2$ vs z at various times during the pulse. One acoustic period is $\simeq 100$ psec. The CO_2 best focus is at $z = 0$.